Target dependence of doubly differential electron-detachment cross sections

Joseph Macek
Department of Physics and Astronomy, University of Nebraska, Lincoln, Nebraska 68588-0111

M. G. Menendez and M. M. Duncan
Department of Physics and Astronomy, University of Georgia, Athens, Georgia 30602
(Received 11 July 1983)

We show that the pronounced structure in the energy spectra of electrons ejected in the forward directions in H^- stripping depends upon the mean excitation energy of the target-gas molecules. The measured spectra for He, Ne, Ar, and CH_3Cl targets is in qualitative agreement with first-Born-approximation calculations.

I. INTRODUCTION

Stripping of H^- by He targets produces secondary-electron distributions peaked at 0° in the laboratory frame.[1] The electron-energy spectra show two peaks,[1] one corresponding to electrons moving at approximately the velocity of the H^- and one slightly lower in energy. The equal velocity peak is expected on the basis of the electron scattering model,[2] but the low-energy peak is not. Born-approximation calculations by Franz, Genoni, and Wright[3] using orthogonalized plane waves for the final states of H^- showed that this second peak reflected considerable structure in the transition form factor of H^-. This explanation was confirmed[4] by subsequent Born-approximation calculations using more realistic wave functions, which incorporated the known low-energy phase shift of the s-wave component of the H^- continuum, for the final H^- states. Since no experiments involving the low-energy spectrum of H^-, in particular the elastic scattering of electrons from H targets, reveal such structure, it is desirable to investigate the effect systematically. The purpose of this study was to determine the conditions that make such structure observable with He targets.

We argue that the structure is due to interference between s- and p-wave components of the final outgoing electron wave function. Since such interference is present in many processes involving H^- our interest here is to see why it is observed in only one reaction. A key feature is that the stripping of H^- to produce low-energy electrons in the H^- frame is associated with excitation of the target.[4] This introduces a target effect via the average excitation energy of the stripping gas. Part of our investigations deal with experimental and theoretical studies of the target effect.

The interference term is proportional to the cosine of the angle between the momentum-transfer vector $\vec{K}$ and the outgoing-electron wave vector $\vec{k}$. When little energy is transferred from relative to internal motion, the vector $\vec{K}$ is predominantly perpendicular to the incident beam direction in the frame in which H^- is at rest. Then $\hat{K}\cdot\hat{k}=\cos(\phi-\phi')$, where ϕ' is the azimuthal angle of the scattered He (recall that we are working in the H^- frame). Upon integrating over ϕ', we see that the interference term disappears and no structure is observed. Alternatively, when considerable energy is transferred to internal motion, the momentum-transfer vector $\vec{K}$ acquires a component parallel to the incident beam direction and the interference terms are nonzero even after integrating over azimuthal directions. For this reason He, which has the highest excitation energy of all neutral atomic or molecular species, is the most favorable target to exhibit the structure of the low-energy H^- form factor.

Interference between s and p waves, and indeed among the various partial waves plays a significant role in all secondary-electron angular distributions. It usually becomes prominent in the binary-collision region where the momentum is transferred to the secondary electron and produces a peak at $\cos\theta=\Delta E/v$, where ΔE is the inelastic energy loss of the projectile, v is its velocity, and θ is the secondary-electron ejection angle in the H^- frame. This binary-collision peak is reproduced in the plane-wave approximation and appears as the nearly equal velocity peak in the laboratory frame.[4] Thus, more than just interference between s and p waves is needed to accurately describe the structure of the H^- form factor. The additional feature needed is the low-energy phase shift of the s-wave electrons. Since the phase shift is close to 180°, the interference term enters in with a negative sign and results in destructive interference where the plane-wave approximation predicts constructive interference. The destructive interference introduces a valley in the three-dimensional plot[4] of the H^- form factor versus k and θ which cuts across the binary-collision maxima. The resulting structure is observed as two peaks in the laboratory-frame secondary-electron spectra.[4] We have studied the structure of the secondary-electron spectra for a variety of electron ejection angles, incident ion velocities, and atomic and molecular targets, thereby varying the average excitation energy of the target. Details of the calculations are given in Sec. II, the experiment is described in Sec. III, and the results are discussed in Sec. IV. Atomic units are used throughout unless otherwise indicated.

II. THEORY

We evaluate the doubly differential cross section (DDCS) for the reaction

$$H^- + T \rightarrow H + e^- + T \tag{1}$$

in the frame in which H^- is at rest. It was shown in Ref. 4 that for the low-energy electrons of interest here, the target T is left in an excited state and the DDCS is well approximated by

$$\frac{d^2\sigma}{dE\,d\Omega} = A \int_{K_{\min}}^{K_{\max}} J(K) d\ln K \tag{2}$$

where A is given by

$$A = 32\pi kC/v \ , \tag{3}$$

and C is a constant depending upon the target. The quantity $J(K)$ is the H^- transition form factor $\epsilon^{H^-}(\vec{K})$ averaged over azimuthal angles. Our calculations use Schwinger variational wave functions and are described in detail in Ref. 4. In this section we show how the interference between s and p waves depends upon the average ionization potential of the target.

The cross section in Eq. (2) depends upon the mean ionization potential through $K_{\min}$,

$$K_{\min} = \Delta E/v \ , \tag{4}$$

where ΔE is the sum of the mean excitation energy of the target, the electron affinity of H^-, and the kinetic energy of the outgoing electron. Now $K_{\min}$ enters explicitly in the limits of integration, and implicitly through $J(K)$. Since $J(K)$ peaks in physically accessible regions of K, the dependence on the limit of integration is weak and does not account for the target dependence of the DDCS, rather the implicit dependence is significant.

To extract this dependence, we make a partial-wave expansion of $\epsilon^{H^-}(\vec{K})$

$$\epsilon^{H^-}(K) = \sum_l \exp(-i\delta_l)\epsilon^l(K) P_l(\hat{K}\cdot\hat{k}) \ , \tag{5}$$

where δ_l is the lth-partial-wave phase shift of the secondary electron. Each coefficient $\epsilon^l(K)$ is real and independent of the direction of K. The argument of the Legendre polynomials is given in terms of the polar coordinates θ_f, ϕ_f, and θ, ϕ of the outgoing momentum $\vec{k}_f$ and the electron momentum $\vec{k}$, respectively, by the equation

$$\vec{K}\cdot\vec{k} = k_i\cos\theta - k_f[\cos\theta_f\cos\theta - \sin\theta_f\sin\theta\cos(\phi_f - \phi)] \ . \tag{6}$$

Since the structure occurs in the meV electron-energy range, we need only keep the $l=0$ and $l=1$ terms in Eq. (5). Substituting Eq. (6) into the definition of $J(K)$ and averaging over ϕ_f we obtain

$$J(K) = |\epsilon^0(K)|^2 + (2\pi)^{-1}\int |\epsilon^1(K) P_1(\hat{K}\cdot\hat{k})|^2 dd_f + 2\cos(\delta_0 - \delta_1)\epsilon^0(K)\epsilon^1(K)(k_i - k_f\cos\theta_f)\cos\theta/K \ . \tag{7}$$

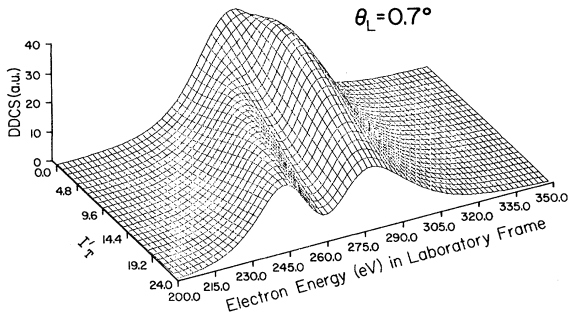

FIG. 1. Plot of doubly differential cross section for H^- stripping vs electron energy and mean excitation energy I_T' of the target for an electron ejection of 0.7° in the laboratory frame and an incident H^- energy of 0.5 MeV.

To a good approximation we have

$$k_i - k_f\cos\theta_f = K_{\min} \tag{8}$$

so that the interference term in Eq. (7) is proportional to the ratio $K_{\min}/K$. When $K_{\min}$ is small compared to the value of K where $J(K)$ peaks, which was seen to be of order of $K=0.5$ in Ref. 4, the interference term vanishes and the DDCS shows no structure. Alternatively, when $K_{\min}$ is large the interference term is significant. Since the minimum momentum transfer can be large for low-energy electrons only if the mean excitation energy of the target is large, we expect that the structure in the DDCS will be most pronounced for He and less pronounced in other noble gases.

Figure 1 shows a plot of the DDCS versus laboratory electron energy and average excitation energy of the target for 0.5-MeV H^- and secondary-electron ejection angle δ^- of 0.7° in the laboratory frame. The DDCS exhibit only shows one peak for low-average excitation energies, but shows two peaks above $\Delta E = 10$ eV, in accord with our qualitative analysis.

The zero-average excitation energy limit in Fig. 1 corresponds to no target excitation; however, it was shown in Ref. 4 that this channel contributes negligibly to the DDCS in the region of interest here. This was proven only for targets with no electric dipole moments. For targets with electric dipole moments, the target form factor can be written

$$\epsilon^T(\vec{K}) = Z_T + i\vec{D}\cdot\vec{K} + \bar{\epsilon}^T(\vec{K}) \ , \tag{9a}$$

where

$$\bar{\epsilon}^T(\vec{K}) = \left\langle \psi \left| \left[\sum_{i=1}^{Z_T} [\exp(i\vec{K}_L\cdot\vec{r}) - i\vec{K}\cdot\vec{r}_i] - Z_T \right] \right| \psi \right\rangle \ . \tag{9b}$$

Upon expanding the exponential for small $\vec{K}$ and using the definition (in atomic units)

$$\vec{D} = \sum_{i=1}^{Z_T} \langle \psi | \vec{r}_i | \psi \rangle \ ,$$

we have that

$$\bar{\epsilon}^{T}(\vec{K}) \sim K^2 \quad \text{as } K \to 0 \, .$$

The DDCS corresponding to no target excitation is, in the H^- frame,

$$\frac{d\sigma}{d\Omega} = \frac{4k}{v^2} \int_0^{2\pi} \int_{K_{\min}}^{K_{\max}} |\epsilon^{H^-}(\vec{K})|^2 |Z_T - \epsilon^{T}(\vec{K})|^2 \times K^{-3} dK \, d\varphi_f \, . \tag{10}$$

Substituting Eq. (9a) into Eq. (10), averaging over all orientations of the dipole and neglecting $\bar{\epsilon}^{T}(\vec{K})$ gives

$$\frac{d\sigma}{d\Omega} = A \int_{K_{\min}}^{K_{\max}} J(K) d\ln K \, , \tag{11}$$

where A is given by

$$A = (32\pi k/v^2)(\vec{D}^2/3) \, . \tag{12}$$

Since Eq. (11) has the same form as Eq. (2) one can study the structure for zero excitation energy by using targets with permanent dipole moments. One must recognize, of course, that there will also be components corresponding to target excitation.

III. EXPERIMENT

The experimental arrangement used to measure the electron-energy spectra of the detached electrons in the extreme forward direction is described elsewhere.[5] The following experimental conditions are pertinent to these measurements.

(i) The analyzer angular acceptance $\Delta\theta_L$ was $\pm 0.4°$.

(ii) The analyzer energy resolution $\Delta E/E$ in the laboratory system was ± 0.015.

(iii) For laboratory electron velocities near that of the ion velocity, the $\Delta\theta_L$ and ΔE in the laboratory give rise to an energy spread in the H^- frame of 60 meV for experiments at 0.5 MeV.

(iv) The earth's magnetic field was compensated to about 10 mG throughout the region of the cross beam and analyzer.

(v) The uncertainty in the location of the absolute energy was estimated to be less than 2%.

The experimental curves shown below have been corrected for the linear energy dependence of the analyzer resolution.

The principal motivation of these measurements was to observe the general behavior of the target, velocity, and angular dependence of the structure of the electron-energy spectra in order to compare with theoretical predictions. Such a comparison does not require that measurements be made at 0° since the structure persists at larger angles. Thus the procedure used previously to obtain data between 0° and 0.5° was not necessary. The data presented here are for angles of 0.7° and greater where there was no problem associated with the incident beam hitting surfaces in the analyzer. Furthermore, the analyzer was not calibrated for the mode used in these measurements. The energy scale used in the figures was established using the design value of the analyzer constant for this mode of operation. However, a previous calibration of this analyzer, operated in a slightly different mode gave a value for the analyzer constant within 1.5% of the design value for that mode of operation. Hence, we must quote an uncertainty in the energy scale between 1% and 2%.

Only relative cross sections were measured. For ease of comparison with the calculations several normalization schemes were used. See individual figure captions.

IV. DISCUSSION

The central result of our theoretical considerations is the strong sensitivity of the structure in the spectral of electrons in the forward direction to the minimum momentum transfer. This is illustrated in the plot of the calculated DDCS versus electron energy and target-ionization potential in Fig. 1. We use Eqs. (10) and (13) of

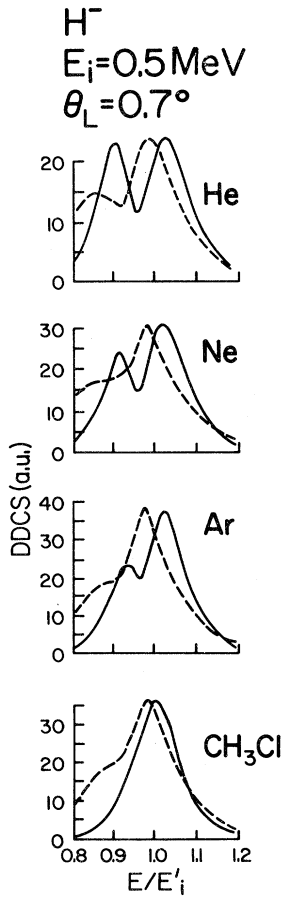

FIG. 2. Comparison of experimental and theoretical cross sections for different targets. The experimental data are shown as dashed curves and the theoretical calculations are shown as solid curves. For ease of comparison the experimental curves have been normalized individually such that the experimental "equal velocity" peak has approximately the same value as the calculated cross section for the equal velocity peak. The DDCS scale is from the calculations. E_i' is the electron energy corresponding to an electron velocity equal to the incident ion velocity.

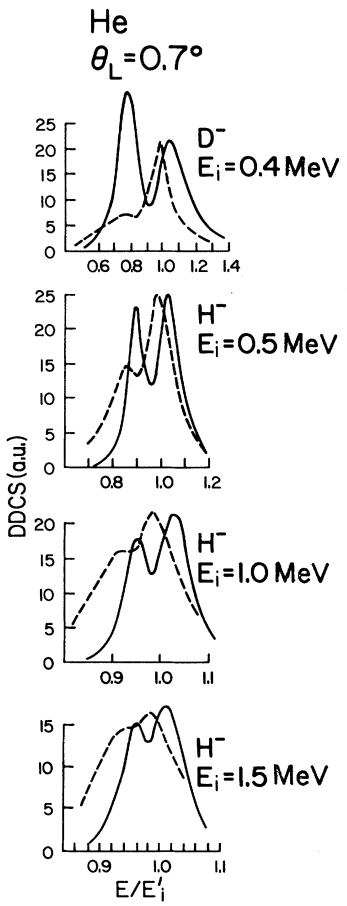

FIG. 3. Comparison of experimental and theoretical cross sections for different ion velocities. (See Fig. 2 for additional information.)

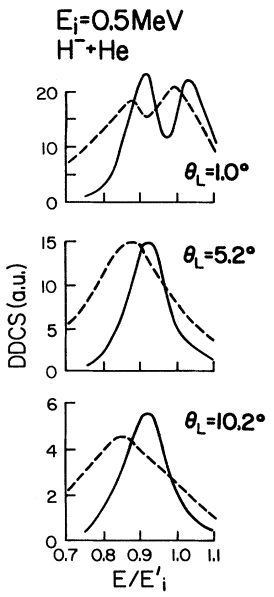

FIG. 4. Comparison of the experimental and theoretical angular dependences of electron-energy spectra for H^--He collisions at 0.5 MeV. For ease of comparison a normalization procedure has again been used. The relative experimental data have been normalized to calculations at 5.2° only by setting the maximum experimental value of the DDCS equal to the calculated maximum value.

Ref. 4 in all calculations. Helium targets, with the highest ionization potential show distinct double-peaked structure while the structure is less pronounced for lower I. Because this qualitative feature relates to very general behavior of $J(K)$ it is likely to appear in better calculations of the DDCS. This is supported by the measurements in Fig. 2 where the minimum momentum transfer is varied by varying the target, and in Fig. 3 by varying v while holding the target fixed. Note that the double-peaked structure diminishes with decreasing minimum momentum transfer, although the agreement is by no means quantitative. This is not surprising, since such structure is sensitive to s- and p-wave phase shifts and our model only incorporates an approximate s-wave phase shift and a zero p-wave phase shift. We can safely conclude that the double-peak structure does arise from the interference of s and higher partial-wave contributions to the stripping cross section.

The disappearance of the structure with increasing electron ejection angle is also confirmed by the data shown in Fig. 4, but the calculated peak position increasingly diverges from experiment with increasing angles. Alternatively, the electron scattering model (ESM) gives a good description of integrated electron spectra versus scattering angle for angles greater than 45°. At large angles target excitation is no longer dominant, but higher-order interactions of the electron with the target, including the polarization of the target, are dominant. This requires second- and higher-order terms in the Born expansion, and indi-

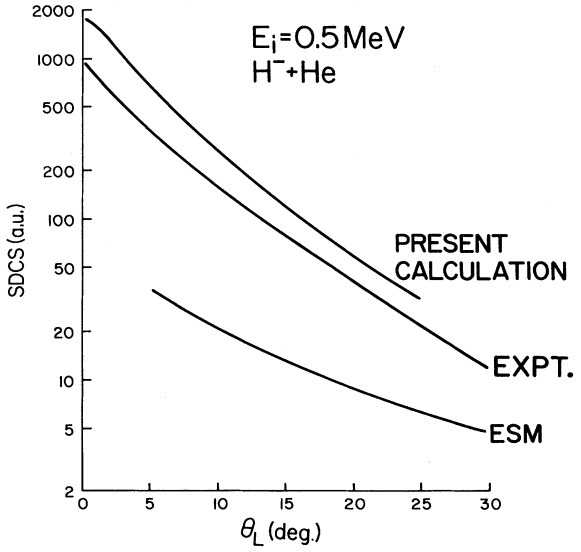

FIG. 5. Comparison of the single-differential cross section for the H^--He collision at 0.5 MeV. Shown are the present calculations compared to both an experimental curve and a curve calculated using an electron scattering model (ESM); both are taken from Ref. 1.

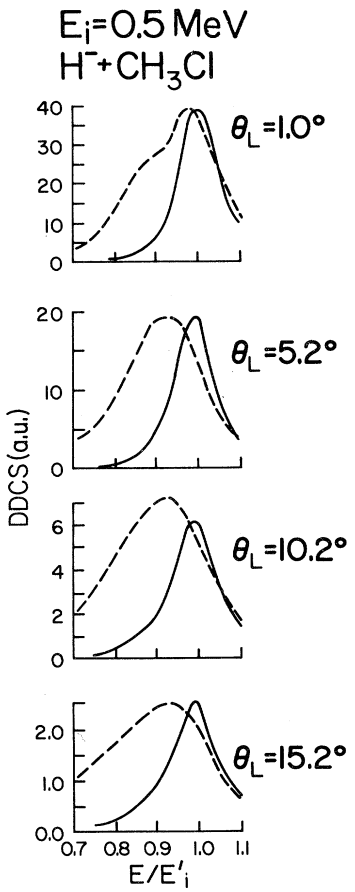

FIG. 6. Comparison of the experimental and theoretical angular dependences of electron-energy spectra for H^- collisions with the polar molecule CH_3Cl at 0.5 MeV. (See caption of Fig. 4.)

cates a possible future direction for theoretical work. The approach of the experimental and first-Born-approximation cross sections to the (ESM) cross section is shown in Fig. 5. Both the first-Born-approximation cross section and experiment approach the ESM predictions, but the variation of the cross section integrated over electron energy with angle follows the present calculation. Apparently the discrepancy between ESM predictions and experiment below 30° noted in Ref. 5 is due to omission of the target-excitation channel.

The data in Fig. 6 are for CH_3Cl target molecules, which have permanent dipole moments. The theory in this instance takes $I=0$ as explained in Sec. II. The first feature to note is the structure in the DDCS at 1° which is similar to the structure in Ar. In order for such structure to appear the minimum momentum transfer must be of the order of 10 eV/v, indicating that some target excitation occurs. Our calculations do not incorporate such excitation and accordingly show no structure. The calculations also considerably underestimate the number of electrons under the peak at all angles; however, the variation of the peak height is surprisingly well reproduced. This can perhaps be understood on the basis of the electron scattering model. The scattering in this case is from a permanent electric dipole which is reasonably well described by the first Born approximation even for relatively low-electron energies. Now our Born-approximation stripping cross sections incorporate the electron dipole scattering in first order, thus the angular dependence should approximate the angular dependence of the electron scattering model. In addition there appears to be a component corresponding to target excitation not included in the theory. Inclusion of such a channel represents a possible direction for future work. Since electron scattering from electric dipoles is quite probable, it may also be of interest to measure the total stripping cross section for such targets.

Since completing this work we have learned of recent calculations by Wright, Genoni, and Franz[6] which are relevant here. Firstly, Wright *et al.*[6] demonstrate that the mean excitation energy of He is more nearly equal to 35 eV than to the 22 eV which follows from the prescription of Briggs and Taulbjerg[7] that we have used. This changes the quantitative results, but does not affect the qualitative conclusions. More importantly, they show that processes in which the H atom is left in the 2s state contribute substantially to the second peak, but not to the first. Both of these effects alter the relative magnitudes of the two peaks, but do not change our qualitative conclusions regarding target dependence.

ACKNOWLEDGMENTS

Support for this research by U.S. Air Force Office for Scientific Research Grant No. AFOSR-81-0129 and National Science Foundation Grant No. PHY-82-03400 is gratefully acknowledged.

[1]M. G. Menendez and M. M. Duncan, Phys. Rev. A 20, 2327 (1979).
[2]D. Burch, H. Wieman, and W. B. Ingalls, Phys. Rev. Lett. 30, 823 (1973).
[3]M. R. Franz, L. A. Wright, and T. C. Genoni, Phys. Rev. A 24, 1135 (1981).
[4]N. Maleki and J. Macek, Phys. Rev. A 26, 3198 (1982).
[5]M. G. Menendez, M. M. Duncan, F. L. Eisele, and B. R. Junker, Phys. Rev. A 15, 80 (1977).
[6]L. A. Wright, T. C. Genoni, and M. R. Franz, Bull. Am. Phys. Soc. 28, 799 (1983).
[7]J. S. Briggs and K. Taulbjerg, *Structure and Collisions of Ions and Atoms,* Vol. 5 of *Topics in Current Physics,* edited by I. A. Sellin (Springer, Berlin, 1978), p. 113.